Princeton Plasma Physics Laboratory

PPPL-5273

The Role of Far-Field RF Sheaths in SOL Losses of HHFW Power on NSTX, and Implications for Near-Field Studies of ICRF Antennae

R. J. Perkins, J.C. Hosea, M.A. Jaworski, R.E. Bell, N. Bertelli,
G. J. Kramer, L. Roquemore, G. Taylor, and J.R. Wilson

July 2016

Prepared for the U.S.Department of Energy under Contract DE-AC02-09CH11466.

Princeton Plasma Physics Laboratory
Report Disclaimers

Full Legal Disclaimer

Trademark Disclaimer

PPPL Report Availability

Princeton Plasma Physics Laboratory:

http://www.pppl.gov/techreports.cfm

Office of Scientific and Technical Information (OSTI):

http://www.osti.gov/scitech/

Related Links:

U.S. Department of Energy

U.S. Department of Energy Office of Science

U.S. Department of Energy Office of Fusion Energy Sciences

The Role of Far-Field RF Sheaths in SOL Losses of HHFW Power on NSTX, and Implications for Near-Field Studies of ICRF Antennae

R. J. Perkins,[1] J. C. Hosea,[1] M. A. Jaworski,[1] R. E. Bell,[1] N. Bertelli,[1]
G. J. Kramer,[1] L. Roquemore,[1] G. Taylor,[1] and J. R. Wilson[1]

[1] *Princeton Plasma Physics Laboratory, Princeton, New Jersey, USA*

Abstract

Radio-frequency (RF) rectification is an important sheath phenomenon for wave heating of plasma in fusion devices and is proposed to be the mechanism responsible for converting high-harmonic fast-wave (HHFW) power in the National Spherical Torus eXperiment (NSTX) into a heat flux to the divertor. RF rectification has two aspects: current rectification and voltage rectification, and, while the latter is emphasized in many application, we demonstrate the importance of current rectification in analysis of the NSTX divertor during HHFW heating. When rectified currents are accounted for in first-principle models for the heat flux to the tiles, we predict a sizeable enhancement for the heat flux in the presence of an RF field: for one case studied, the predicted heat flux increases from 0.103 MW/m^2 to 0.209 MW/m^2. We also demonstrate how this rectification scales with injected HHFW power by tracking probe characteristics during a HHFW power ramp; the rectified current may be clamped at a certain level. This work is important for minimizing SOL losses of HHFW power in NSTX-U but may also have implications for near-field studies of ICRF antennae: ignoring rectified current may lead to underestimated heat fluxes and overestimated rectified voltages.

I. INTRODUCTION

Radio-frequency (RF) rectification is a non-linear process by which RF electric fields enhance certain aspects of the sheath. The RF fields tend to increase the average electron current flowing through the sheath; we refer to this effect as current rectification. The plasma potential *may*, in turn, increase in order to offset, or screen, the enhanced electron current; in which case the potential is said to be rectified. We propose three potential sheath responses to an impressed RF voltage, illustrated in Fig. 1: (i) an increased electron current with little to no change in plasma potential, (ii) an increase in plasma potential just enough to completely cancel the increased electron current, or (iii) partial screening, in which both rectified a electron current and plasma potential are present. While response (ii) is assumed in many applications of RF rectification, we find that, in the divertor of the National Spherical Torus eXperiment (NSTX) during high-harmonic fast-wave (HHFW) heating, probe data clearly indicate the presence of rectified currents, indicating either response (i) or (iii) but not (ii). We predict, for NSTX conditions, that the increase in heat flux to the underlying surface due to RF rectification is greater for response (i) than (ii). Also, we follow the evolution of a probe characteristic during an HHFW power ramp, giving the degree of rectification as a function of RF voltage. The primary motivation for this work is to quantify the role of RF rectification in scrape-off layer (SOL) losses of HHFW power on NSTX, but there may be implications for the impact of RF rectification at ion-cyclotron range of frequencies (ICRF) antennas.

RF rectification plays a somewhat unusual and unique role in the NSTX divertor during HHFW heating. The HHFW system launches fast waves at frequencies well above the ion-cyclotron frequency and is intended to provide electron heating and current drive [1], but HHFW experiments have shown a significant loss of HHFW power directly to the SOL [2]. During such experiments, bright and hot spirals form on the upper and lower divertor (Fig. 2); infrared (IR) cameras measures a heat flux within these spirals up to 2 MW/m^2 for an applied RF power of 1.8 MW [3], while up to 60% of the coupled HHFW power is estimated to be missing from the core plasma. In Ref. [4], we proposed that RF rectification is the mechanism responsible for converting wave power into a heat flux [4], with the RF sheaths being driven by enhanced wave fields due to cavity-like modes in the SOL [5, 6]. This constitutes an instance of a far-field sheath [7], where propagating waves intercept a material

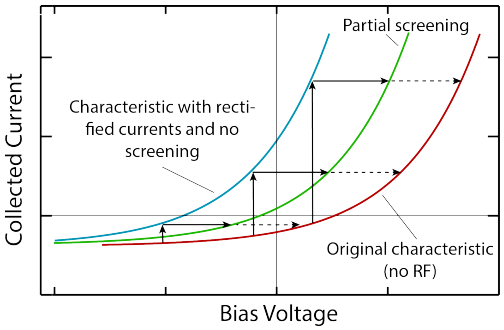

FIG. 1. An illustration of the potential response of a probe IV characteristic to RF rectification. The red rightmost curve represents the original IV characteristic without RF effects. The vertical solid lines show the action of rectified electron currents, lifting the characteristic to the blue leftmost curve. The horizontal solid lines show the action of an increased plasma potential, shifting the characteristic to the right to the green middle curve, partially cancelling the rectified current. The dashed horizontal arrows represent full screening, when the plasma potential increases enough to fully cancel the rectified currents.

surface some distance away from the antenna. However, unlike the more conventional picture in which the sheath is established by wave power gradually leaving the core in regimes of low single-pass absorption [7, 8], RF rectification in the NSTX divertor occurs prior to wave energy reaching the core, as NSTX has a high absorption rate for such waves [9]. It is of great importance for the HHFW program to determine the scaling of the heat flux driven by RF rectification as a function of the RF potential across the sheath.

RF rectification has a broad scope of application in the fusion:

1. RF rectification has been incriminated for the increased production of impurities that often accompany ICRH [10–12], as the rectified sheath voltage may accelerate ions to sufficient energies to enhance sputtering.

2. RF rectification threatens antenna components with premature demise due either to erosion of antenna components via ion bombardment and also overheating due to hot spots, or regions of enhanced heat flux [13–15].

3. RF rectification has been hypothesized to explain modifications to the scrape-off layer (SOL) during ICRF operation [16–18].

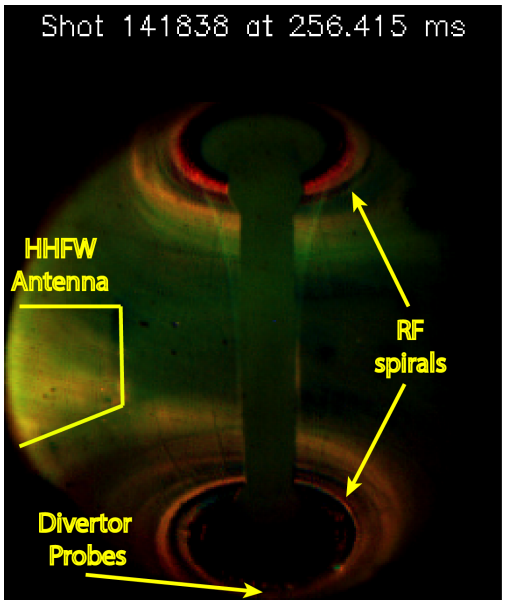

FIG. 2. Fast camera image of NSTX during HHFW heating for shot 141838, an H-mode plasma with 1.2 MW of HHFW power with no neutral beam injection. Time of image is 256.4 ms with a background subtraction of eight frames starting at 215.2 ms. HHFW antenna, HHFW, spiral, and divertor probe positions are indicated.

4. RF rectification presents a potential power sink for RF wave power [7] both for regimes of poor single-pass absorption and the NSTX case of prompt loss.

A large portion of the work on RF sheaths focuses on enhanced ion bombardment due to its potential for impurity production. Also, early consideration of the heat flux to the antenna due to RF rectification only incorporated the rectified voltage (ion bombardment) contribution [10], a practice still in use for studies of heat loads at antennas [15, 19–22] and also for far-field sheaths [23]. This paper focuses on the role of the rectified electron current, its effect on the heat flux, and its relation to the rectified voltage. Although our primary application is far-field sheath dissipation, this work may impact studies of antenna hot spots, as we calculate that the heat flux due to rectified currents scales differently than that due to rectified voltages. Also, for a measured V_{RF}, neglecting rectified currents will tend to overestimate the predicted change in rectified sheath voltage, potentially impacting sputtering studies. We note that DC currents due to ICRF operation were observed long ago [16, 24, 25] and are still observed on modern antennas [11]. Recent modeling has also begun to incorperate DC currents [26].

II. ION AND ELECTRON CONTRIBUTIONS TO RF-DRIVEN SHEATH HEAT FLUXES

This section will develop the formulas needed to make concrete the concepts of rectified current and rectified voltage introduced above. These formulas will also be used to seperate the heat flux due to RF rectification into ion-bombardment and thermal-electron components. The two different scalings of each component will be discussed.

It is convenient to assume a Maxwellian electron distribution, which leads to the usual IV characteristic:

$$I(V) = \frac{I_{\rm sat}}{1-\delta_e}\left(-1 + e^{(V-V_{fl}^{noRF})/T_e}\right). \tag{1}$$

I^{sat} is the ion saturation current. δ_e is the coefficient of secondary electron emission, which can be ignored for grazing incidence magnetic fields [27] (such as occurs in the divertor) but might be important for antenna components. We set $\delta_e = 0$ for convenience. V_{fl}^{noRF} is the floating potential without RF. Voltages are defined relative to vessel potential.

We consider two modifications to Eq. (1). First, we superimpose over the bias voltage V an RF voltage $V_{RF}\cos\omega t$ and average. This produces the rectified electron current:

$$I_{RF}^{-}(V) = I^{sat} I_0\left(\frac{V_{RF}}{T_e}\right)\exp\left(\frac{V-V_{fl}}{T_e}\right), \tag{2}$$

with I_0 the modified Bessel function [28]. Second, we assume that the plasma potential, V_{pl} changes by an amount ΔV_{pl} in response to the RF rectified currents and add ΔV_{pl} to the floating potential V_{fl}^{noRF}. This assumes that the common textbook relationship between plasma potential and floating potential [29]:

$$V_{fl}^{noRF} = V_{pl} - \frac{1}{2}\ln\left(2\pi\frac{m_e}{m_i}\left(1+\frac{T_i}{T_e}\right)\right) \tag{3}$$

continues to hold in the presence of the RF fields. We plan to test this assumption in future HHFW experiments. Adding these two modifications to Eq. (1) yields

$$I(V) = \frac{I_{\rm sat}}{1-\delta_e}\left(-1 + I_0\left(\frac{V_{RF}}{T_e}\right)e^{(V-V_{fl}^{noRF}-\Delta V_{pl})/T_e}\right). \tag{4}$$

Also, if we define

$$V_{fl}^{RF} = T_e \ln I_0\left(\frac{V_{RF}}{T_e}\right), \tag{5}$$

then Eq. (4) can be cast is the form

$$I(V) = \frac{I_{\rm sat}}{1-\delta_e}\left(-1 + e^{(V+V_{fl}^{RF}-V_{fl}^{noRF}-\Delta V_{pl})/T_e}\right). \tag{6}$$

Let us now interpret Eq. (6) in terms of the different potential response of a sheath to the RF fields. Case (i) above assumes no change in plasma potential, $\Delta V_{pl} = 0$. The probe IV characteristic is effectively shifted negative by an amount V_{fl}^{RF}. At any bias voltage V, the probe collects more electron current than without the RF. In case (ii), we assume $\Delta V_{pl} = V_{fl}^{RF}$. The means that, for bias V below $V_{pl} - V_{RF}$, the probe charactersitic is unaltered, and the probe collects the same current as it would without RF. Finally, case (iii) corresponds to an intermediate situation with $0 < \Delta V_{pl} < V_{fl}^{RF}$. Cases (i) and (ii) are complimentary, and we can drawn a circuit analogy in which the RF rectification plays the role of a non-ideal voltage (or current) source. In the perfect screening case the plasma-sheath system acts as though it has infinite impedance to ground, allowing no rectified current to flow in exchange for an elevated mean (rectified) voltage. The case of no screening behaves as though there was zero impedance to ground and conducts the rectified current with no change in voltage.

The heat flux Q_{RF} to a surface biased at potential V with a superimposed RF voltage is given by [4]

$$\begin{aligned} Q_{RF}(V) &= -I^{sat}(V - V_{pl}^{noRF} + \Delta V_{pl}) + 2.5 T_i I^{sat} + \ldots \\ &\quad \frac{2}{1-\delta_e} I^{sat} T_e I_0\left(\frac{V_{RF}}{T_e}\right) e^{(V - V_{fl}^{noRF} - \Delta V_{pl})/T_e} \qquad (7) \\ &= -J^{sat} V + 2.5 T_i J^{sat} + \frac{2}{1-\delta_e} J_{RF}^{-} T_e, \qquad (8) \end{aligned}$$

Equation 7 is straightforward extension of the no-RF case [29]. The first term of Eq. (7) is the energy gained by the ions as they fall through the sheath potential. Since this term is linear in V, the RF voltage simply averages out, but this term contributes when $\Delta V_{pl} \neq 0$. The second term is the energy flux (flow plus thermal) of the ions at the sheath edge, which is independent of V and is rather set by the Bohm sheath criteria. It does not get directly modified by the RF potential. The last term is the thermal energy flux from the electrons and is proportional to the rectified electron current, Eq. (2).

The heat flux due to RF rectification is

$$\begin{aligned} \Delta Q_{RF} &= \Delta V_{pl} I^{sat} + \ldots \\ &\quad \frac{2 I^{sat} T_e}{1-\delta_e} e^{(V - V_{fl}^{noRF})/T_e} \left(I_0\left(\frac{V_{RF}}{T_e}\right) e^{-\Delta V_{pl}/T_e} - 1 \right). \qquad (9) \end{aligned}$$

The thermal heat flux from the ions drops out from Eq. (9). Clearly, the larger ΔV_{pl}, the greater the ion bombardment term at the expense of the electron thermal contribution. In

the case of perfect screening, the electron term of Eq. (7) does not contribute to ΔQ_{RF}, as there is no change in electron current, and

$$\Delta Q_{RF,rv} = \Delta V_{pl} J^{sat} = T_e J_{sat} \ln\left(I_0\left(\frac{V_{RF}}{T_e}\right)\right) \tag{10}$$

with the subscript "rv" denoting "rectified voltage." This equation is frequently used in the ICRF community [15, 19–21] for the contribution of heat flux to a surface due to RF rectification or even for far-field sheath dissipation [23] and assumes that ion bombardment dominates. The validity of this assumption will be discussed in Sec. IV. In the case of no screening, $\Delta V_{pl} = 0$, so the ion term of Eq. (7) does not contribute to ΔQ_{RF}, leaving

$$\Delta Q_{RF,rc} = \frac{2J^{sat}T_e}{1-\delta_e} e^{(V-V_{fl})/T_e}\left(I_0\left(\frac{V_{RF}}{T_e}\right) - 1\right). \tag{11}$$

For large V_{RF}, this heat flux scales nearly exponentially with V_{RF}, indicating that, at some point, the plasma must begin to screen the rectified currents, and the heat flux scaling will transition over to Eq. (10).

Equations (11) and (10) scale differely as a function of V_{RF}/T_e, although direct comparison requires knowing the additional parameter in Eq. (11): $(V - V_{fl}^{noRF})/T_e$. In general, for $V_{RF} \gg T_e$, Eq. (10) yields a ΔQ much greater than Eq. (11), as Eq. (11) asymptotes to $\exp(V_{rf}/T_e)/(V_{RF}/T_e)^{1/2}$ while Eq. (10) asymptotes to V_{RF}/T_e. It is also not too difficult to show that, for $(V - V_{fl}^{noRF})/T_e \geq 0$, Eq. (11) produces a greater ΔQ_{RF} than Eq. (10) for all V_{RF}. However, if $(V - V_{fl}^{noRF})/T_e < 0$, there is a value of V_{RF}/T_e for which Eq. (11) and Eq. (10) gives the same ΔQ_{RF} and below which Eq. (10) exceeds Eq. (11). The NSTX divertor probes considered in Sec. III have $(V - V_{fl}^{noRF})/T_e > 0$, so that Eq. (11) always produces the larger heat flux. Equations (11) and (10) represent idealized cases as discussed above, and the actual ΔQ_{RF} should fall somewhere inbetween.

III. APPLICATION TO SOL LOSSES IN THE NSTX DIVERTOR

The previous section presents different scalings for Q_{RF} versus V_{RF} based on whether one assumes rectified currents or rectified voltages. Swept Langmuir probe data from the divertor of NSTX during HHFW heating, however, rules out the possibility of complete current screening via voltage rectification. For all cases analyzed in Ref. [4], a downward shift in floating potential was observed with little change in electron temperature for a

Shot	P_{RF} [MW]	T_e [eV]	V_{fl} [V]	$V_{fl,RF}$ [V]	$\Delta\gamma_{RF}$	$\Delta\gamma_{RF,fl}$	Q_{noRF} [MW/m^2]	$\Delta Q_{RF,rc}$ [MW/m^2]	$\Delta Q_{RF,rv}$ [MW/m^2]
141899	1.5	13.5	4	-20	7.3	1.8	0.1	0.21	0.13
141836	1.1	30	5	-23	2.5	0.92	0.35	0.49	0.5
141830	0.55	22.5	1	-10	2.8	0.49	0.37	0.44	0.38

TABLE I. Predictions based on divertor Langmuir probe data. both as the heat flux Q and the sheath heat transmission coefficient $\gamma = Q/J_{sat}T_e$.

probe that was located underneath the RF spiral compared to a nearby probe that was not underneath the spiral. At vessel potential, $V = 0$, the probe under the spiral draws more DC electron current with HHFW than without HHFW. Clearly, the plasma has not completely screened the rectified current, although the possibility of incomplete screening will be discussed in Sec. IV. Note that non-zero currents to divertor tiles are observed in tokamak divertors without RF [30]; in NSTX, the current path may close through the vessel to the private flux region [31]. Table I summarizes the analysis of the Langmuir probes for the shots analyzed in Ref. [4] and also evaluates the heat flux for the cases of zero current screening, Eq. (11), and full current screening, Eq. (10), for comparison. V_{RF} is computed using Eq. (5) assuming that the observed change in floating potential is entirely due to V_{fl}^{RF} with no change in plasma potential $\Delta V_{pl} = 0$. In all cases considered, the assumption of zero current screening results in higher heat fluxes than the assumption of perfect screening.

In this paper, we adopt a different approach and analyze characteristics from a single probe (Probe 1, radius 63.82 cm) during the 10 ms HHFW power ramp. The sweep rate is 1 kHz, so this ramp presents the opportunity to observe the probe characteristic evolution with increasing RF voltage. Unfortunately, the individual IV characteristics have large fluctuations, presumably from SOL/divertor turbulence [32, 33], so that the uncertainty in the fit parameters tends to obscure the signs of RF rectification. To obtain more reliable fits, we average each sweep with its two neighboring sweeps. This is a necessary compromise between time resolution and accuracy of the fitting procedure. We also compute the standard deviation of collected current at each bias voltage for each average for use in the fitting procedure so that points with large variance are weighted less. Unfortunately, with the small sample for each average, this procedure tends to produces a few points with exceptionally

low variance, so that the χ^2-minimization routine is dominated by fitting to this handful of points. We thus set a minimum variance of 2.5 mA, which avoids this issue while still giving less weights to those points with large variance. Finally, it is known that, even without RF, including bias voltages well above the floating potential tends to skew the fit to higher temperatures [34]. The HHFW heating primarily lowers probe floating potential, bringing more of the high-bias region into the sweep range. Also, an RF voltage causes the probe, at any bias V, to sample from $V - V_{RF}$ to $V + V_{RF}$; potentially distorting the high-bias region if it samples voltages exceeding the plasma potential [28] or even regions of suppressed electron collection [4]. Finally, the high-bias region is most susceptible to error from averaging consecutive sweeps when V_{fl} is changing in time. For these reasons, we only include bias voltages less than $V_{fl} + 25$ V in each fit. An exponential curve of the form in Eq. (1) is then fit to the averaged characteristic using standard χ^2-minimization routines. The averaged characteristics over the full sweep range and accompanying fits over the restricted range are shown for four time slices in Fig. 3 for shot 141838, an H-mode discharge with 1.1 MW of HHFW power and no neutral beam injection.

Figure 4 plots the fitted parameters against $\langle P_{RF} \rangle$, the average RF power during the interval of averaging. Comparing Fig. 4.a to 4.b, the HHFW power primarily lowers V_{fl} with less pronounced and systematic effects of T_e and I_{sat}, consistent with conclusions drawn in Ref. [4]. This favors the hypothesis of a cavity-like mode driving the SOL losses of HHFW over the alternative hypothesis of parasitic plasma heating in front of the antenna. Figure 4 plots the fitted floating potential against the mean RF power; V_{fl} rises relatively sharply with HHFW power but then appears to be clamped around -10 V. We speculate that the plasma begins to screen the rectified currents, preventing V_{fl} from dropping any more. However, changes in discharge conditions and evolution of the magnetic equilibrium, shifting the spiral location, can contribute as well. For this discharge, the 1.1 MW of applied HHFW power is more than a significant perturbation to the target plasma. Figure 4.c shows the computed value of V_{RF} obtained inverting Eq. (5) and assuming that $\Delta V_{pl} = 0$. V_{RF} initially rises with $\langle P_{RF} \rangle$ and then levels off, but it is unlikely that V_{RF} is clamped like ΔV_{fl}. Instead, the assumption of $\Delta V_{pl} = 0$ perhaps becomes invalid, causing an underestimation of V_{RF}. We might anticipate that V_{RF} is proportional to the antenna voltage, which generally scales as $P_{RF}^{1/2}$. We can roughly fit a square-root function to the first four data points, as shown in Fig. 4.c, but the data quickly deviates from this trend at larger powers. In Fig. 4.d, we

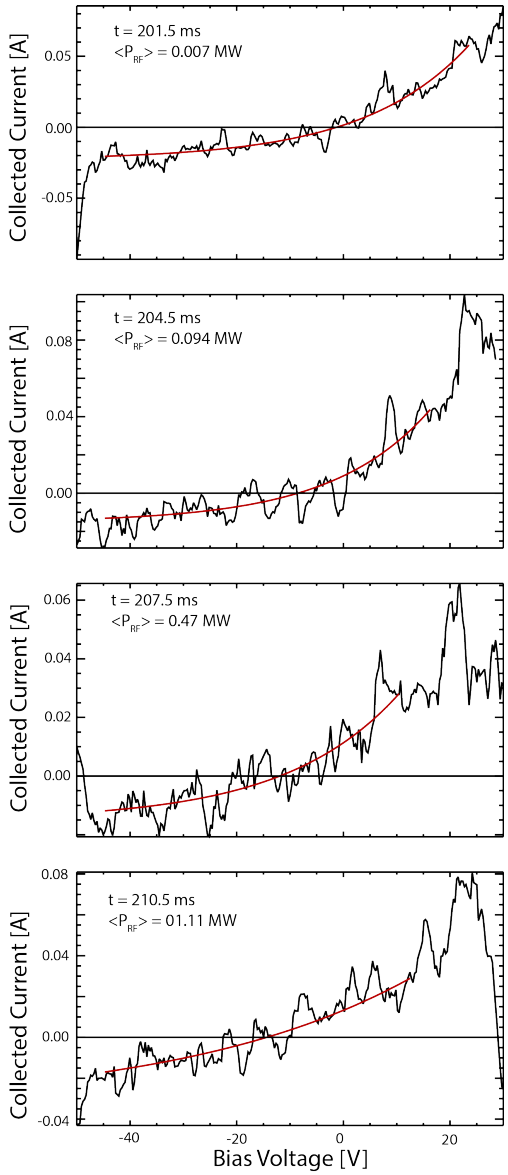

FIG. 3. Averaged probe characteristics taken during the 10 ms ramp HHFW. Despite averaging, sizable fluctuations are still visible. However, a clear downward shift in floating potential is seen as the HHFW power increases.

compute ΔQ_{RF} based on both Eqs. (11) and Eq. (10). As in Table I, the assumption of no-screening always yields a larger heat flux via current rectification.

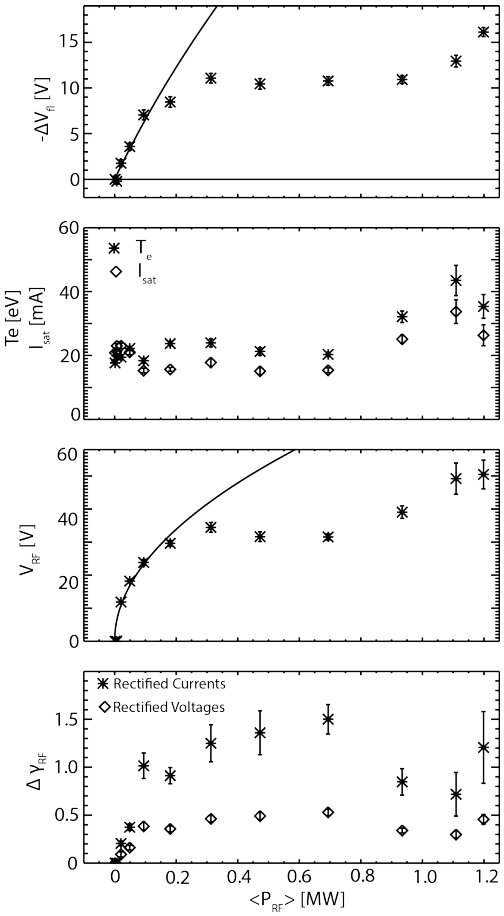

FIG. 4. Fit results from averaged IV characteristics during the HHFW ramp, plotted as a function of the average HHFW power during the averaging window. (a) Negative of the floating potential, (b) electron temperature and ion saturation current, (c) V_{RF}, assuming no change in plasma potential, and (e) ΔQ_{RF} expressed as the sheath heat transmission factor $\gamma = Q/T_e I^{Sat}$, calculated both for the assumption of zero screening and full screening.

IV. DISCUSSION

In Sec. III, we mentioned the possibility of partial screening: the change in floating potential observed on the probe, $\Delta V_{fl,ob}$, is a combined negative shift due to RF rectification plus a positive change in plasma potential:

$$\Delta V_{fl,ob} = V_{fl}^{noRF} - V_{fl}^{RF} + \Delta V_{pl}. \tag{12}$$

$\Delta V_{fl,ob}$ is given from the probe characteristic, but ΔV_{pl} and V_{RF} are unknown, as the Langmuir probes are incapable of resolving the plasma potential. Assuming $\Delta V_{pl} = 0$, as done in

Sec. III, gives the smallest V_{RF} and also the smallest ΔQ_{RF} that is consistent with the data. For the latter, note that, in Eq. (9), the thermal electron contribution is independent of the actual value of ΔV_{pl} because it is proportional to the electron current, which is measured and fixed. The ion bombardment contribution, which is proportional to ΔV_{pl}, is minimized when $\Delta V_{pl} = 0$. As noted in Ref. [4], our best extrapolation of heat flux to the probe location indicates that the heat flux is larger than what is predicted with the probe sheath theory, which may suggest that partial screening is in action, but this is conjecture at this point. Note that the arguments used in this paragraph, should not be confused with those in the last paragraph of Sec. II. Here, we are working with the constraint of a fixed probe floating potential given by probe measurements, whereas in Sec. III we essentially fixed V_{RF}.

The NSTX swept probes do not, for practical reasons, sweep high enough to probe the plasma potential, so obtaining ΔV_{pl} may require dedicated techniques, such as emissive probes [35]. Alternatively, a floating probe nearby could complement the swept probe measurements: the floating probe draws no rectified current, so that one could compute V_{RF} directly from Eq. (5) and estimate ΔV_{pl} from Eq. (12). An alternate approach being pursued on NSTX-U is to directly measure the RF component of the swept Langmuir probe signal to compute V_{RF} will retaining the DC measurements.

While rectified currents are important in the analysis of the NSTX divertor, their impact at an ICRF antenna is less clear. We anticipate that the plasma will screen the rectified current to a greater degree at the antenna because V_{RF} should be much larger there, and the rectified current, Eq. (2), scales nearly exponentially with V_{RF}. This would lead to very large (unrealistic) currents that, at some point, must be screened. Also, certain antenna components such as the Faraday screen bars are magnetically connected to other nearby components and act as a double probe system that could limit rectified currents [36]. That being said, rectified current to and from ICRF antennas have been observed [11, 24, 25]. The outer portions of the antenna limiter, for instance, have long magnetic connection lengths, so that cross-field diffusion can play a more important role, and V_{RF} there may be smaller than at the straps or Faraday screen. Moreover, secondary electron emission may exacerbate the effect of rectified currents, as the angle of incidence on the limiter may not be low enough to suppress the secondaries. As argued in Secs. II and III, for a given V_{RF} the presence of rectified currents impacts calculations of both the heat flux to surfaces and the rectified voltage; assuming full screening would underestimate the heat flux and overestimate ion

bombardment.

V. CONCLUSIONS

An RF potential across a sheath will drive a rectified current, a rectified voltage, or both, and the heat flux due to rectification is predicted to scale in different fashions for each case. In the divertor of NSTX during HHFW heating, rectified currents grow and then appear to saturate with increasing HHFW power. The predicted heat fluxes are substantially larger with the rectified current than those assuming rectified voltages. It is possible that similar conclusions may be reached for certain components of an ICRF antenna itself. This investigation will be continued on NSTX-U with dedicated divertor Langmuir probes equipped with electronics to measure the RF component of the signal, and also with midplane probes at the antenna. Also, IR thermography will be available for these probes, allowing validation of the scaling of heat flux with rectification.

This work was supported by DOE Contract No. DE-AC02-09CH11466.

---

[1] M. Ono, "High harmonic fast waves in high beta plasmas," *Physics of Plasmas*, vol. 2, no. 11, pp. 4075–4082, 1995.

[2] J. Hosea, R. E. Bell, B. P. LeBlanc, C. K. Phillips, G. Taylor, E. Valeo, J. R. Wilson, E. F. Jaeger, P. M. Ryan, J. Wilgen, H. Yuh, F. Levinton, S. Sabbagh, K. Tritz, J. Parker, P. T. Bonoli, R. Harvey, and N. Team, "High harmonic fast wave heating efficiency enhancement and current drive at longer wavelength on the National Spherical Torus Experimental," *Phys. Plasmas*, vol. 15, no. 5, 2008.

[3] J. C. Hosea, R. E. Bell, E. Feibush, R. W. Harvey, E. F. Jaeger, B. P. LeBlanc, R. Maingi, C. K. Phillips, L. Roquemore, P. M. Ryan, G. Taylor, K. Tritz, E. J. Valeo, J. Wilgen, J. R. Wilson, and the NSTX Team, "Recent fast wave coupling and heating studies on NSTX, with possible implications for ITER," *AIP Conference Proceedings*, vol. 1187, no. 1, pp. 105–112, 2009.

[4] R. J. Perkins, J. C. Hosea, M. A. Jaworski, J.-W. Ahn, A. Diallo, R. E. Bell, N. Bertelli, S. Gerhardt, T. K. Gray, G. J. Kramer, B. P. LeBlanc, A. McLean, C. K. Phillips, M. Podestà,

L. Roquemore, S. Sabbagh, G. Taylor, and J. R. Wilson, "The contribution of radio-frequency rectification to field-aligned losses of high-harmonic fast wave power to the divertor in the National Spherical Torus eXperiment," *Phys. Plasmas*, vol. 22, no. 4, 2015.

[5] N. Bertelli, E. Jaeger, J. Hosea, C. Phillips, L. Berry, S. Gerhardt, D. Green, B. LeBlanc, R. Perkins, P. Ryan, G. Taylor, E. Valeo, and J. Wilson, "Full wave simulations of fast wave heating losses in the scrape-off layer of NSTX and NSTX-U," *Nuclear Fusion*, vol. 54, no. 8, p. 083004, 2014.

[6] N. Bertelli, E. Jaeger, J. Hosea, C. Phillips, L. Berry, P. Bonoli, S. Gerhardt, D. Green, B. LeBlanc, R. Perkins, C. Qin, R. Pinsker, R. Prater, P. Ryan, G. Taylor, E. Valeo, J. Wilson, J. Wright, and X. Zhang, "Full wave simulations of fast wave efficiency and power losses in the scrape-off layer of tokamak plasmas in mid/high harmonic and minority heating regimes," *Nuclear Fusion*, vol. 56, no. 1, p. 016019, 2016.

[7] J. R. Myra, D. A. D'Ippolito, and M. Bures, "Far field sheaths from waves in the ion cyclotron range of frequencies," *Physics of Plasmas*, vol. 1, no. 9, 1994.

[8] C. Petty, F. Baity, J. deGrassie, C. Forest, T. Luce, T. Mau, M. Murakami, R. Pinsker, P. Politzer, M. Porkolab, and R. Prater, "Fast wave current drive in H mode plasmas on the DIII-D tokamak," *Nucl. Fusion*, vol. 39, no. 10, p. 1421, 1999.

[9] C. Phillips, R. Bell, L. Berry, P. Bonoli, R. Harvey, J. Hosea, E. Jaeger, B. LeBlanc, P. Ryan, G. Taylor, E. Valeo, J. Wilgen, J. Wilson, J. Wright, H. Yuh, and the NSTX Team, "Spectral effects on fast wave core heating and current drive," *Nucl. Fusion*, vol. 49, no. 7, p. 075015, 2009.

[10] M. Bureš, J. Jacquinot, M. Stamp, D. Summers, D. Start, T. Wade, D. D'Ippolito, and J. Myra, "Assessment of beryllium faraday screens on the JET ICRF antennas," *Nuclear Fusion*, vol. 32, no. 7, p. 1139, 1992.

[11] Vl.V. Bobkov, F. Braun, R. Dux, A. Herrmann, L. Giannone, A. Kallenbach, A. Krivska, H. Müller, R. Neu, J.-M. Noterdaeme, T. Pütterich, V. Rohde, J. Schweinzer, A. Sips, I. Zammuto, and the ASDEX Upgrade Team, "Assessment of compatibility of ICRF antenna operation with full W wall in ASDEX upgrade," *Nucl. Fusion*, vol. 50, no. 3, p. 035004, 2010.

[12] A. N. James, D. Brunner, B. Labombard, C. Lau, B. Lipschultz, D. Miller, M. L. Reinke, J. L. Terry, C. Theiler, G. M. Wallace, D. G. Whyte, S. Wukitch, and V. Soukhanovskii, "Imaging of molybdenum erosion and thermography at visible wavelengths in Alcator C-Mod ICRH and

LHCD discharges," *Plasma Physics and Controlled Fusion*, vol. 55, no. 12, p. 125010, 2013.

[13] L. Colas, L. Costanzo, C. Desgranges, S. Brémond, J. Bucalossi, G. Agarici, V. Basiuk, B. Beaumont, A.Bècoulet, and F. Nguyen, "Hot spot phenomena on Tore Supra ICRF antennas investigated by optical diagnostics," *Nuclear Fusion*, vol. 43, no. 1, p. 1, 2003.

[14] K. Saito, T. Mutoh, R. Kumazawa, T. Seki, Y. Nakamura, N. Ashikawa, K. Sato, M. Shoji, S. Masuzaki, T. Watari, H. Ogawa, H. Takeuchi, H. Kasahara, F. Shimpo, G. Nomura, M. Yokota, C. Takahashi, A. Komori, Y. Zhao, J. Yoon, and J. Kwak, "ICRF long-pulse discharge and interaction with a chamber wall and antennas in LHD," *Journal of Nuclear Materials*, vol. 363365, pp. 1323 – 1328, 2007. Proceedings of the 17th International Conference on Plasma-Surface Interactions in Controlled Fusion Device.

[15] P. Jacquet, L. Colas, M.-L. Mayoral, G. Arnoux, V. Bobkov, M. Brix, P. Coad, A. Czarnecka, D. Dodt, F. Durodie, A. Ekedahl, D. Frigione, M. Fursdon, E. Gauthier, M. Goniche, M. Graham, E. Joffrin, A. Korotkov, E. Lerche, J. Mailloux, I. Monakhov, C. Noble, J. Ongena, V. Petrzilka, C. Portafaix, F. Rimini, A. Sirinelli, V. Riccardo, Z. Vizvary, A. Widdowson, K.-D. Zastrow, and JET-EFDA Contributors, "Heat loads on JET plasma facing components from ICRF and LH wave absorption in the SOL," *Nucl. Fusion*, vol. 51, no. 10, p. 103018, 2011.

[16] G. V. Oost, R. V. Nieuwenhove, R. Koch, A. Messiaen, P. Vandenplas, R. Weynants, K. Dippel, K. Finken, Y. Lie, A. Pospieszczyk, U. Samm, B. Schweer, R. Conn, W. Corbett, D. Goebel, and R. Moyer, "Invited paper: ICRF/Edge physics research on TEXTOR," *Fusion Engineering and Design*, vol. 12, no. 1, pp. 149 – 170, 1990.

[17] J. M. Noterdaeme and G. V. Oost, "The interaction between waves in the ion cyclotron range of frequencies and the plasma boundary," *Plasma Physics and Controlled Fusion*, vol. 35, no. 11, p. 1481, 1993.

[18] M. Bècoulet, L. Colas, S. Pécoul, J. Gunn, P. Ghendrih, A. Bècoulet, and S. Heuraux, "Edge plasma density convection during ion cyclotron resonance heating on Tore Supra," *Physics of Plasmas*, vol. 9, no. 6, 2002.

[19] L. Colas, P. Jacquet, G. Agarici, C. Portafaix, M. Goniche, and JET-EFDA contributors, "RF-sheath heat flux estimates on Tore Supra and JET ICRF antennae. Extrapolation to ITER," *AIP Conference Proceedings*, vol. 1187, no. 1, pp. 133–136, 2009.

[20] L. Colas, D. Milanesio, E. Faudot, M. Goniche, and A. Loarte, "Estimated RF sheath power

fluxes on ITER plasma facing components," *Journal of Nuclear Materials*, vol. 390391, pp. 959 – 962, 2009. Proceedings of the 18th International Conference on Plasma-Surface Interactions in Controlled Fusion Devices.

[21] P. Jacquet, F. Marcotte, L. Colas, G. Arnoux, V. Bobkov, Y. Corre, S. Devaux, J.-L. Gardarein, E. Gauthier, M. Graham, E. Lerche, M.-L. Mayoral, I. Monakhov, F. Rimini, A. Sirinelli, and D. V. Eester, "Characterisation of local ICRF heat loads on the JET ILW," *Journal of Nuclear Materials*, vol. 438, Supplement, pp. S379 – S383, 2013. Proceedings of the 20th International Conference on Plasma-Surface Interactions in Controlled Fusion Devices.

[22] D. A. D'Ippolito and J. R. Myra, "Low-power fast wave antenna loading as a radiofrequency sheath diagnostic," *Phys. Plasmas*, vol. 3, no. 1, pp. 420–426, 1996.

[23] D. A. D'Ippolito and J. R. Myra, "A radio-frequency sheath boundary condition and its effect on slow wave propagation," *Phys. Plasmas*, vol. 13, no. 10, p. 102508, 2006.

[24] R. V. Nieuwenhove and G. V. Oost, "Experimental evidence for sheath effects at the ICRF antenna and ensuing changes in the plasma boundary during ICRF on TEXTOR," *Journal of Nuclear Materials*, vol. 162, pp. 288 – 291, 1989.

[25] R. V. Nieuwenhove and G. V. Oost, "Experimental study of sheath currents in the scrape-off layer during ICRH on TEXTOR," *Plasma Physics and Controlled Fusion*, vol. 34, no. 4, p. 525, 1992.

[26] L. Colas, J. Jacquot, S. Heuraux, E. Faudot, K. Crombe, V. Kyrytsya, J. Hillairet, and M. Goniche, "Self consistent radio-frequency wave propagation and peripheral direct current plasma biasing: Simplified three dimensional non-linear treatment in the wide sheath asymptotic regime," *Physics of Plasmas*, vol. 19, no. 9, 2012.

[27] S. Mizoshita, K. Shiraishi, N. Ohno, and S. Takamura, "Plasma-surface interactions in controlled fusion devices secondary electron emission from solid surface in an oblique magnetic field," *Journal of Nuclear Materials*, vol. 220, pp. 488 – 492, 1995.

[28] A. Boschi and F. Magistrelli, "Effect of a R.F. signal on the characteristic of a Langmuir probe," *Il Nuovo Cimento*, vol. 29, no. 2, pp. 487–499, 1963.

[29] P. C. Stangeby, *The Plasma Boundary of Magnetic Fusion Devices*. Plasma Physics Series (Taylor and Francis Group), 2000.

[30] D. Donovan, D. Buchenauer, J. Watkins, A. Leonard, C. Wong, M. Schaffer, D. Rudakov, C. Lasnier, and P. Stangeby, "Experimental measurements of the particle flux and sheath

power transmission factor profiles in the divertor of DIII-D," *Journal of Nuclear Materials*, vol. 438, Supplement, pp. S467 – S471, 2013. Proceedings of the 20th International Conference on Plasma-Surface Interactions in Controlled Fusion Devices.

[31] J. C. Hosea, R. J. Perkins, M. A. Jaworski, G. J. Kramer, J.-W. Ahn, R. E. Bell, N. Bertelli, S. Gerhardt, T. K. Gray, B. P. LeBlanc, R. Maingi, C. K. Phillips, L. Roquemore, P. M. Ryan, S. Sabbagh, G. Taylor, K. Tritz, J. R. Wilson, and S. Zweben, "Predictions of V_{RF} on a Langmuir probe under the RF heating spiral on the divertor floor on NSTX-U," in *41st European Physical Society Conference on Plasma Physics*, 2014.

[32] J. A. Boedo, J. R. Myra, S. Zweben, R. Maingi, R. J. Maqueda, V. A. Soukhanovskii, J. W. Ahn, J. Canik, N. Crocker, D. A. D'Ippolito, R. Bell, H. Kugel, B. Leblanc, L. A. Roquemore, D. L. Rudakov, and the NSTX Team, "Edge transport studies in the edge and scrape-off layer of the National Spherical Torus Experiment with Langmuir probes," *Physics of Plasmas*, vol. 21, no. 4, p. 042309, 2014.

[33] S. J. Zweben, R. R. Myra, W. M. Davis, D. A. D'Ippolito, T. K. Gray, S. M. Kaye, B. P. LeBlanc, R. J. Maqueda, D. A. Russell, D. P. Stotler, and the NSTX-U Team, "Blob structure and motion in the edge of NSTX," *Plasma Phys. and Controlled Fusion*, vol. 58, p. 044007, 2016.

[34] J. A. Tagle, P. C. Stangeby, and S. K. Erents, "Errors in measuring electron temperatures using a single langmuir probe in a magnetic field," *Plasma Physics and Controlled Fusion*, vol. 29, no. 3, p. 297, 1987.

[35] M. J. Martin, J. Bonde, W. Gekelman, and P. Pribyl, "A resistively heated CeB_6 emissive probe," *Review of Scientific Instruments*, vol. 86, no. 5, p. 053507, 2015.

[36] F. Perkins, "Radiofrequency sheaths and impurity generation by ICRF antennas," *Nuclear Fusion*, vol. 29, no. 4, p. 583, 1989.

PPPL PRINCETON PLASMA PHYSICS LABORATORY

Princeton Plasma Physics Laboratory
Office of Reports and Publications

Managed by
Princeton University

under contract with the
U.S. Department of Energy
(DE-AC02-09CH11466)

P.O. Box 451, Princeton, NJ 08543
Phone: 609-243-2245
Fax: 609-243-2751

E-mail: publications@pppl.gov

Website: http://www.pppl.gov